

Eigenbasis of the Evolution Operator of 2-Tessellable Quantum Walks

Yusuke Higuchi,¹ Renato Portugal,² Iwao Sato,³ Etsuo Segawa⁴

¹ Mathematics Laboratories, College of Arts and Sciences, Showa University,
Fujiyoshida, Yamanashi 403-0005, Japan

² National Laboratory of Scientific Computing - LNCC,
Av. Getúlio Vargas 333, Petrópolis, RJ, 25651-075, Brazil

³ Oyama National College of Technology,
Oyama, Tochigi 323-0806, Japan

⁴ Graduate School of Education Center, Yokohama National University,
Hodogaya, Yokohama, 240-8501, Japan

Abstract

Staggered quantum walks on graphs are based on the concept of graph tessellation and generalize some well-known discrete-time quantum walk models. In this work, we address the class of 2-tessellable quantum walks with the goal of obtaining an eigenbasis of the evolution operator. By interpreting the evolution operator as a quantum Markov chain on an underlying multigraph, we define the concept of quantum detailed balance, which helps to obtain the eigenbasis. A subset of the eigenvectors is obtained from the eigenvectors of the double discriminant matrix of the quantum Markov chain. To obtain the remaining eigenvectors, we have to use the quantum detailed balance conditions. If the quantum Markov chain has a quantum detailed balance, there is an eigenvector for each fundamental cycle of the underlying multigraph. If the quantum Markov chain does not have a quantum detailed balance, we have to use two fundamental cycles linked by a path in order to find the remaining eigenvectors. We exemplify the process of obtaining the eigenbasis of the evolution operator using the kagome lattice (the line graph of the hexagonal lattice), which has symmetry properties that help in the calculation process.

1 Introduction

The interest of the scientific community on quantum walks has been increasing unremittingly since the first papers of quantum walks on graphs, such as [6, 1]. This interest seems to be based on at least three reasons: (1) the quantum walk is useful to simulate complex physical systems [13, 4], (2) it is an important tool to build new quantum algorithms [22, 2, 29], and (3) it can be implemented directly in laboratories independently of quantum computers [7, 3]. Besides those physical and computational aspects, the mathematical aspects of the quantum walk are very rich and have been the focus of many papers [26, 10, 27].

A quantum walk is defined on a discrete space, which is modeled by a graph. On the other hand, its time evolution can be either continuous or discrete. There are many attempts to prove the equivalence between the continuous-time and discrete-time approaches, which are successful only at asymptotic limits or on restricted settings [24, 5, 18]. The continuous-time version comes basically in one form, whose evolution operator is local and is obtained from

the graph's adjacency or Laplacian matrix. In this case, the spectral analysis of the graph Laplacian [11] helps to understand the quantum dynamics. The discrete-time versions have evolution operators that are the product of at least two local operators, and the most general models are (1) the coined model [1], (2) Szegedy's model [29], and (3) the staggered model [21]. An extensive comparison of those models is performed in [15]. In the discrete-time case, there is no relation between the eigenvectors of the graph Laplacian and the eigenvectors of the evolution operator.

In this work, we focus on 2-tessellable quantum walks defined on a set of graphs that can be characterized in many ways, for instance, (1) the set of graphs whose clique graphs are 2-colorable, or (2) the set of graphs that are line graphs of bipartite multigraphs. To obtain the evolution operator of a 2-tessellable quantum walk, we need to find two tessellations \mathcal{T}_1 and \mathcal{T}_2 whose union covers the edges of the graph. A tessellation is a partition of the vertex set into cliques, called polygons or tiles. For instance, $\mathcal{T}_1 = \{\alpha_1, \alpha_2, \dots, \alpha_m\}$ is a tessellation of a graph $G = (V, E)$ if each α_ℓ is a clique, $\alpha_\ell \cap \alpha_j = \emptyset$ when $\ell \neq j$, and $\cup_{\ell=1}^m \alpha_\ell = V$. G is 2-tessellable if $E(\mathcal{T}_1 \cup \mathcal{T}_2) = E(G)$. After finding the tessellations, we define two subspaces \mathcal{A} and \mathcal{B} spanned by the polygons of tessellations α and β , respectively. Using orthogonal projections on these subspaces, there is a standard procedure to obtain self-adjoint unitary operators H_1 and H_2 associated with the tessellations \mathcal{T}_1 and \mathcal{T}_2 [21]. The evolution operator of the quantum walk is $U_\theta = -e^{i\theta_2 H_2} e^{i\theta_1 H_1}$, where θ_1, θ_2 are angles and $i = \sqrt{-1}$. In this work, we address the case $\theta_1 = \theta_2 = \theta$ [20].

In order to find the eigenvalues and eigenvectors of the evolution operator of a 2-tessellable quantum walk, we interpret U_θ as a quantum Markov chain [9] on the edges of an underlying multigraph G_{un} , whose line graph is the original graph, that is, $G = L(G_{\text{un}})$. We define the notion of quantum detailed balance using the amplitudes of the polygons and an (+1)-eigenvector of a matrix T , whose biadjacent matrix is the discriminant of the polygons of tessellations \mathcal{T}_1 and \mathcal{T}_2 . T is a double discriminant matrix and is a self-adjoint operator. We say that a quantum Markov chain is reversible when T has an (+1)-eigenvector, which is called a reversible eigenfunction of T . A classical Markov chain is obtained from the quantum chain and the classical detailed balance conditions are obtained from the square modulus of the quantum detailed balance conditions. When T has a quantum detailed balance, the reversible eigenfunction is the only (+1)-eigenvector of T , which means that in the quantum case, the invariant state is always a reversible eigenstate and vice versa, different from the classical Markov chain, whose transition matrix may have a stationary probability distribution even in the irreducible case.

In the staggered model, the Hilbert space is spanned by the vertex set. We split the Hilbert space as a direct sum of $(\mathcal{A} + \mathcal{B})$ and $(\mathcal{A} + \mathcal{B})^\perp$. The eigenvectors of U_θ in $(\mathcal{A} + \mathcal{B})$ are inherited from the eigenvectors of T . On the other hand, the eigenvectors of U_θ in $(\mathcal{A} + \mathcal{B})^\perp$ are obtained from the fundamental cycles of the underlying multigraph G_{un} . The definition of fundamental cycles relies on the concept of a spanning tree, which is a subgraph of G_{un} that is a tree and includes all vertices of G_{un} [8]. Adding one edge to the spanning tree creates a cycle, which is called fundamental cycle. The number of fundamental cycles is equal to the number of edges of G_{un} not in the spanning tree. If T has a quantum detailed balance, there is an eigenvector of U_θ with support on each fundamental cycle, whose expression is described in this work. The dimension of $(\mathcal{A} + \mathcal{B})^\perp$ is the first Betti number in this case. If T does not have a quantum detailed balance, we have to use two fundamental cycles c_0 and c_1 in order to obtain an eigenvector. If c_0 and c_1 do not have common vertices, we have to link them with a path, and the support of the eigenvector is the cycle-path subgraph. The dimension of $(\mathcal{A} + \mathcal{B})^\perp$ in this case is the first Betti number minus 1. The eigenvectors in $(\mathcal{A} + \mathcal{B})^\perp$ play an important

role in determining the efficiency of search algorithms on finite graphs.

We use the kagome lattice [28, 25, 16] as an example to show the techniques created in this work because this lattice has interesting symmetries. The dynamic of the staggered quantum walk on the kagome lattice, which is an infinite graph, reduces to a 2-tessellable staggered walk on a triangle, which is the quotient graph of the kagome lattice. The quantum Markov chain is defined on the underlying graph of the quotient graph and is nonreversible. We show how to use the method based on the fundamental cycles to find the eigenvectors in $(\mathcal{A} + \mathcal{B})^\perp$.

This work generalizes Ref. [29], which introduced the notion of Markov chain-based quantum walks, in many aspects: (1) We address forms of quantum walks that were not addressed in [29]. In fact, Szegedy's model is a subset of quantum walks obtained from the set of 2-tessellable quantum walks if we set $\theta = \pi/2$ and employ a graph whose underlying graph does not have multiedges, (2) Ref. [29] does not describe the eigenvectors associated with the cycle-path space $(\mathcal{A} + \mathcal{B})^\perp$, and (3) Ref. [29] does not describe the quantum detailed balance conditions, which have been proposed for quantum walks in this work, as far as we know. This work generalizes Ref. [14] in two directions: (1) We consider the staggered model with Hamiltonians with a generic θ while Ref. [14] addressed only the case $\theta = \pi/2$, and (2) we obtain a complete eigenbasis while Ref. [14] missed a subset of eigenvectors corresponding to the space $(\mathcal{A} + \mathcal{B})^\perp$. Primitive ideas related to the cycle-path space were first introduced in [23] from the point of view of simple random walks on line and para-line graphs. After that the ideas are applied to the spectral analysis of twisted random walks [11] and twisted Grover walks [10]. The twisted Grover walk on the para-line graph is a special case of the model presented in this work, since there is an equivalence between the Grover walk and the 2-tessellable quantum walk [15]. Here, we have further developed the concept of cycle-path space, which can now be used in a more general setting. The structure of this paper is as follows. In Sec. 2 we define the staggered quantum walk, its evolution operator, and the subspaces spanned by the polygons. In Sec. 3 we obtain the eigenvalues of the evolution operator of 2-tessellable quantum walks. In Sec. 4 we define the quantum detailed balance conditions and obtain an eigenbasis of the evolution operator U_θ of 2-tessellable quantum walks. This section is divided into three subsections, which address the eigenvectors in the following subspaces: $(\mathcal{A} \cap \mathcal{B})$, $(\mathcal{A} + \mathcal{B})$, and $(\mathcal{A} + \mathcal{B})^\perp$. In Section 5 we summarize our results in a theorem. In Section 6 we use the kagome lattice as an example.

2 The 2-tessellable quantum walk

The evolution operator of a staggered quantum walk on a graph $G = (V, E)$ is associated with a graph tessellation cover. A tessellation cover is a set of graph tessellations whose union covers the edge set. The formal definition is as follows [21].

Definition 1. *A graph tessellation \mathcal{T}_1 of $G = (V, E)$ is a partition of the vertex set V into cliques. An edge belongs to the tessellation \mathcal{T}_1 if and only if the edge endpoints belong to the same clique in \mathcal{T}_1 . The set of edges belonging to \mathcal{T}_1 is denoted by $\mathcal{E}(\mathcal{T}_1)$. An element of the tessellation is called a polygon (or tile). The size of a tessellation \mathcal{T}_1 is the number of polygons in \mathcal{T}_1 . A tessellation cover of size k of G is a set of k tessellations $\mathcal{T}_1, \dots, \mathcal{T}_k$ whose union covers the edges, that is, $\cup_{i=1}^k \mathcal{E}(\mathcal{T}_i) = E(G)$. If there is a tessellation cover of size at most k , graph G is called k -tessellable.*

A staggered quantum walk on a k -tessellable graph is called k -tessellable quantum walk. Since this paper addresses 2-tessellable quantum walks, we assume from now on that $k = 2$. A graph is 2-tessellable if and only if its clique graph is 2-colorable [19]. Besides, it is known

that the clique graph of a graph G is 2-colorable if and only if G is the line graph of a bipartite multigraph [17]. Then, throughout this paper, G is the line graph of a bipartite multigraph on which we now define a 2-tessellable quantum walk.

Suppose that $\{\mathcal{T}_1, \mathcal{T}_2\}$ is a tessellation cover of G , where $\mathcal{T}_1 = \{\alpha_1, \alpha_2, \dots, \alpha_m\}$, $\mathcal{T}_2 = \{\beta_1, \beta_2, \dots, \beta_n\}$, where $m = |\mathcal{T}_1|$ and $n = |\mathcal{T}_2|$. Let us assume that $n \geq m$. Generic polygons of \mathcal{T}_1 and \mathcal{T}_2 are denoted by α_i and β_j , respectively. Let \mathcal{H} be the Hilbert space $\ell^2(V)$, that is, \mathcal{H} is spanned by the vertices. The standard basis of \mathcal{H} is denoted by $\{|u\rangle \mid u \in V\}$ which coincides with the delta function on each vertex. We assign a complex-valued unit vector in \mathcal{H} to each polygon: $|\alpha_1\rangle, |\alpha_2\rangle, \dots, |\alpha_m\rangle, |\beta_1\rangle, |\beta_2\rangle, \dots, |\beta_n\rangle$, that is, if $u \notin \alpha_i$, then $\langle u|\alpha_i\rangle = 0$ ($i = 1, \dots, m$), and if $v \notin \beta_j$, then $\langle v|\beta_j\rangle = 0$ ($j = 1, \dots, n$). For any $u \in V$, let $\mathcal{T}_1(u) \in \mathcal{T}_1$ and $\mathcal{T}_2(u) \in \mathcal{T}_2$ be the polygons that include u . A vertex u belongs to exactly two polygons, which we call α_i and β_j . Let $a, b \in \mathbb{C}$ be the functions such that for $u \in \alpha_i \cap \beta_j$,

$$a(u) := \langle u|\alpha_i\rangle; \quad b(u) := \langle u|\beta_j\rangle. \quad (2.1)$$

Let $A : \ell^2(\mathcal{T}_1) \rightarrow \ell^2(V)$ and $B : \ell^2(\mathcal{T}_2) \rightarrow \ell^2(V)$ be $A = [|\alpha_1\rangle \mid \alpha_2\rangle \cdots \mid \alpha_m\rangle]$ and $B = [|\beta_1\rangle \mid \beta_2\rangle \cdots \mid \beta_n\rangle]$, that is, $(Af)(u) = a(u)f(\mathcal{T}_1(u))$ and $(Bg)(u) = b(u)g(\mathcal{T}_2(u))$ for any $u \in V$, $f \in \ell^2(\mathcal{T}_1)$, and $g \in \ell^2(\mathcal{T}_2)$. Then, $(A^\dagger\psi)(\alpha_i) = \langle \alpha_i|\psi\rangle$ and $(B^\dagger\psi)(\beta_j) = \langle \beta_j|\psi\rangle$.

Hamiltonians H_A and H_B associated with tessellations \mathcal{T}_1 and \mathcal{T}_2 , respectively, are defined by

$$H_A = 2AA^\dagger - I_{\mathcal{H}}, \quad (2.2)$$

$$H_B = 2BB^\dagger - I_{\mathcal{H}}. \quad (2.3)$$

Note that AA^\dagger and BB^\dagger are projection operators on

$$\mathcal{A} := \text{span}\{|\alpha_i\rangle \mid i = 1, 2, \dots, m\} = \{Af \mid f \in \ell^2(\mathcal{T}_1)\}, \quad (2.4)$$

$$\mathcal{B} := \text{span}\{|\beta_j\rangle \mid j = 1, 2, \dots, n\} = \{Bg \mid g \in \ell^2(\mathcal{T}_2)\}, \quad (2.5)$$

respectively, and besides

$$A^\dagger A = I_{\ell^2(\mathcal{T}_1)}, \quad B^\dagger B = I_{\ell^2(\mathcal{T}_2)}. \quad (2.6)$$

Then, H_A and H_B are self-adjoint unitary operators, that is, $H_A^2 = H_B^2 = I_{\mathcal{H}}$. The evolution operator of a 2-tessellable quantum walk is defined as [20]

$$U_\theta = -e^{i\theta H_B} e^{i\theta H_A}, \quad (2.7)$$

where $\theta \in (0, \pi)$ is a fixed parameter and a minus sign was added for convenience. The values $\theta = 0$ and π are excluded because the walk is trivial in these cases. In the next sections, we address the problem of finding the eigenvalues and eigenvectors of U_θ .

3 Eigenvalues

Let U_θ be the evolution operator of a 2-tessellable staggered quantum walk on G , as described in Section 2. In this section we obtain the spectrum of U_θ . Let us start with a useful lemma.

Lemma 1. *Let*

$$M = I_{\mathcal{H}} + \frac{b}{a}BB^\dagger, \quad N = I_{\mathcal{H}} - \frac{b}{a+b}BB^\dagger,$$

where a, b are complex numbers. Then, $MN = I$ and

$$\det(M) = \left(\frac{a+b}{a}\right)^n.$$

Besides Lemma 1, the proof of the next theorem uses the fact

$$\det(I_{m_1} - M_1 M_2) = \det(I_{m_2} - M_2 M_1),$$

where M_1 and M_2 are $m_1 \times m_2$ and $m_2 \times m_1$ matrices, respectively.

Theorem 1. *The characteristic polynomial of U_θ is*

$$\det(\lambda I_{\mathcal{H}} - U_\theta) = (\lambda + 1)^{n-m} \left(\lambda + e^{-2i\theta} \right)^{\nu-m-n} \det \left((\lambda + 1)^2 I_m - 4\lambda \sin^2(\theta) A^\dagger B B^\dagger A \right),$$

where $\nu = |V|$.

Proof. Using equation (2.7), we have

$$\det(I_{\mathcal{H}} - u U_\theta) = \det(I_{\mathcal{H}} + u e^{i\theta H_B} e^{i\theta H_A}),$$

where $|u| = 1$. Commuting the order of the matrices inside the determinant, using that $e^{i\theta H_A} = \cos \theta I_{\mathcal{H}} + i \sin \theta H_A$, $e^{i\theta H_B} = \cos \theta I_{\mathcal{H}} + i \sin \theta H_B$, equations (2.2) and (2.3), we obtain

$$\begin{aligned} \det(I_{\mathcal{H}} - u U_\theta) &= \det \left((1 + u e^{-2i\theta}) I_{\mathcal{H}} + 2iu \sin(\theta) e^{-i\theta} B B^\dagger - \right. \\ &\quad \left. 2u \sin^2(\theta) A A^\dagger (2B B^\dagger - (1 + i \cot \theta) I_{\mathcal{H}}) \right). \end{aligned}$$

Factoring out the term $(1 + u e^{-2i\theta})$ and using that the determinant of a matrix product of square matrices equals the product of their determinants, we obtain

$$\begin{aligned} \det(I_{\mathcal{H}} - u U_\theta) &= a^\nu \det \left(I_{\mathcal{H}} - \frac{c}{a} A A^\dagger (2B B^\dagger - (1 + i \cot \theta) I_{\mathcal{H}}) (I_{\mathcal{H}} + \frac{b}{a} B B^\dagger)^{-1} \right) \times \\ &\quad \det \left(I_{\mathcal{H}} + \frac{b}{a} B B^\dagger \right), \end{aligned}$$

where $a = 1 + u e^{-2i\theta}$, $b = 2iu \sin \theta e^{-i\theta}$, and $c = 2u \sin^2 \theta$.

By Lemma 1, we have

$$\det \left(I_{\mathcal{H}} + \frac{b}{a} B B^\dagger \right) = \frac{(a+b)^n}{a^n}.$$

and

$$\left(I_{\mathcal{H}} - \frac{b}{a} B B^\dagger \right)^{-1} = I_{\mathcal{H}} - \frac{b}{a+b} B B^\dagger.$$

Using these identities and equation (2.6), we obtain

$$\begin{aligned} \det(I_{\mathcal{H}} - u U_\theta) &= a^{\nu-n} (a+b)^n \times \\ &\quad \det \left(I_{\mathcal{H}} - \frac{c}{a} A A^\dagger \left(\frac{2a+b+ib \cot \theta}{a+b} B B^\dagger - (1 + i \cot \theta) I_{\mathcal{H}} \right) \right). \end{aligned}$$

Commuting the order of the matrices inside the determinant and factoring out the denominator, we obtain

$$\begin{aligned} \det(I_{\mathcal{H}} - u U_\theta) &= a^{\nu-m-n} (a+b)^{n-m} \times \\ &\quad \det \left((a+c+ic \cot \theta)(a+b) I_m - c(2a+b+ib \cot \theta) A^\dagger B B^\dagger A \right). \end{aligned}$$

Using that $a+b = a+c+ic \cot \theta = 1+u$ and $2a+b+ib \cot \theta = 1$, we obtain

$$\begin{aligned} \det(I_{\mathcal{H}} - u U_\theta) &= (1 + u e^{-2i\theta})^{\nu-m-n} (1+u)^{n-m} \times \\ &\quad \det \left((1+u)^2 I_m - 4u \sin^2(\theta) A^\dagger B B^\dagger A \right). \end{aligned}$$

Setting $u = 1/\lambda$ in the above equation, we obtain the characteristic polynomial of U_θ in terms of the characteristic polynomial of $A^\dagger B B^\dagger A$. \square

The spectrum of U_θ is obtained from the solutions λ of the equation $\det(\lambda I_{\mathcal{H}} - U_\theta) = 0$. We need the next lemma before describing the spectrum of U_θ .

Lemma 2. *Let T be the following $(n + m) \times (n + m)$ matrix:*

$$T = \begin{bmatrix} 0 & A^\dagger B \\ B^\dagger A & 0 \end{bmatrix}.$$

Then,

$$\det(\mu I - T) = \mu^{n-m} \det(\mu^2 I - A^\dagger B B^\dagger A).$$

The next corollary describes the spectrum of U_θ in terms of the spectrum of T .

Corollary 1. *The spectrum of U_θ is*

$$\sigma(U_\theta) = \left\{ e^{2i\phi} \mid \left(e^{2i\phi} + e^{-2i\theta} \right)^{\nu-m-n} \det \left(\frac{\cos \phi}{\sin \theta} I_{n+m} - T \right) = 0 \right\}.$$

Proof. Using Theorem 1 and factoring out $4\lambda \sin^2(\theta)$, the spectrum of U_θ is obtained from equation

$$(\lambda + 1)^{n-m} \left(\lambda + e^{-2i\theta} \right)^{\nu-m-n} \det \left(\frac{(\lambda + 1)^2}{4\lambda \sin^2(\theta)} I_m - A^\dagger B B^\dagger A \right) = 0.$$

Setting $\lambda = e^{2i\phi}$ and $\cos \phi / \sin \theta = \mu$, using the fact that $(\lambda + 1)^2 / (4\lambda) = \cos^2 \phi$, we obtain

$$\left(e^{2i\phi} + e^{-2i\theta} \right)^{\nu-m-n} \mu^{n-m} \det(\mu^2 I - A^\dagger B B^\dagger A) = 0.$$

Using Lemma 2, we obtain $\sigma(U_\theta)$. □

Lemma 2 implies that $\dim(\ker(T)) \geq n - m$ and, since $\cos \phi = \mu \sin \theta$, the 0-eigenvalues of T are associated with the (-1) -eigenvalues of U_θ . Besides, the $(+1)$ -eigenvalues of T are associated with the $(-e^{-2i\theta})$ -eigenvalues of U_θ . Summarizing, the spectrum of U_θ can be described as follows (see Fig. 1):

- (1) $\lambda = -e^{-2i\theta}$ with multiplicity at least $\max\{\nu - m - n, 0\}$.
- (2) There are $\max\{n + m, \nu\}$ eigenvalues $\lambda = e^{2i\phi}$, where $\cos \phi = \mu \sin \theta$ and

$$\mu \in \begin{cases} \sigma(T) & \text{if } n + m \leq \nu, \\ \sigma(T) \setminus \{1\} & \text{if } n + m > \nu, \end{cases}$$

and, in particular, $\lambda = -1$ with multiplicity at least $n - m$.

The multiplicity of $(-e^{-2i\theta})$ depends on the reversibility of T (see Theorem 2). Note that $\nu - m - n < 0$ if and only if $\nu = m + n - 1$. Take for example $G = P_3$ ($P_3 = \bullet \text{---} \bullet \text{---} \bullet$) and $V(G) = \{1, 2, 3\}$ with $\mathcal{T}_1 = \{\{1, 2\}, \{3\}\}$, $\mathcal{T}_2 = \{\{1\}, \{2, 3\}\}$, which has $\nu = 3$ and $m = n = 2$.

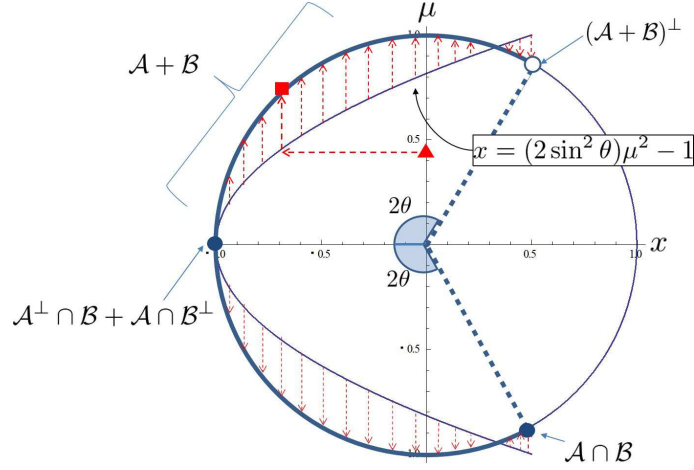


Figure 1: The mapping from $\mu \in \sigma(T)$ to $2\phi \in \sigma(U|_{\mathcal{A}+\mathcal{B}})$: The red triangle \blacktriangle on the μ -axis is mapped to the red square \blacksquare on the unit circle in the complex plane. The blue curve depicted in bold face on the unit circle corresponds to $\mathcal{A}+\mathcal{B}$. The empty point at angle $(\pi - 2\theta)$ corresponds to $(\mathcal{A}+\mathcal{B})^\perp$ and the full point at angle $(\pi + 2\theta)$ corresponds to $\mathcal{A} \cap \mathcal{B}$. The point at angle π mapped from $0 \in \sigma(T)$ corresponds to $\mathcal{A}^\perp \cap \mathcal{B} + \mathcal{A} \cap \mathcal{B}^\perp$.

4 Eigenvectors

In the previous section, we have shown that the self-adjoint matrix T plays a key role in the description of the spectrum of U_θ . In this section, we discuss some extra properties of T in order to obtain the eigenvectors of U_θ . Let \mathcal{K} be the Hilbert space spanned by \mathcal{T}_1 and \mathcal{T}_2 , that is, $\mathcal{K} := \{\psi : \mathcal{T}_1 \sqcup \mathcal{T}_2 \rightarrow \mathbb{C} \mid \|\psi\|^2 < \infty\}$. We employ the standard inner product.

As in Lemma 2, we write $T : \mathcal{K} \rightarrow \mathcal{K}$ as

$$T = \begin{bmatrix} 0 & T_{AB} \\ T_{BA} & 0 \end{bmatrix},$$

where $T_{AB} = A^\dagger B$ and $T_{BA} = T_{AB}^\dagger$. The entries of T are given by $(T_{AB})_{i,j} = \langle \alpha_i | \beta_j \rangle$. Now we define the notions of reversible eigenfunction and quantum detailed balance (QDB) for a pair (a, b) , where a and b are given by Eq. (2.1).

Definition 2. The pair (a, b) obeys the quantum detailed balance conditions if there exists an eigenfunction π of T such that

$$a(u)\pi(\mathcal{T}_1(u)) = b(u)\pi(\mathcal{T}_2(u)),$$

for every $u \in V(G)$. We call this function π a reversible eigenfunction.

We say that T is reversible or T has a quantum detailed balance if there is a pair (a, b) that obeys the QDB conditions. A useful property of the spectrum of T is as follows.

Lemma 3. The spectrum of T obeys $\sigma(T) \subseteq [-1, 1]$.

Proof. Let $f \oplus g \in \ker(\lambda I - T)$. Then,

$$\begin{aligned} |\lambda^2|^2 \|f\|^2 &= \|T_{AB}T_{BA}f\|^2 \leq \langle B^\dagger Af, B^\dagger Af \rangle \\ &= \langle Af, BB^\dagger Af \rangle \\ &\leq \langle Af, Af \rangle \\ &= \|f\|^2. \end{aligned}$$

Since T is self-adjoint and $\lambda^2 \leq 1$, the result follows. \square

Define an underlying bipartite multigraph $G_{\text{un}} = (V_{\text{un}}, E_{\text{un}})$ whose vertex set is $V_{\text{un}} = \mathcal{T}_1 \sqcup \mathcal{T}_2$ and two vertices are adjacent if and only if $|\alpha \cap \beta| > 0$ for $\alpha \in \mathcal{T}_1$ and $\beta \in \mathcal{T}_2$ and the number of multiple edges is given by $|\alpha \cap \beta|$. The adjacency matrix of G_{un} is obtained in the following way. Let A' and B' be the matrices obtained from A and B by replacing the nonzero entries by 1, respectively. The adjacency matrix is

$$T' = \begin{bmatrix} 0 & (A')^T B' \\ (B')^T A' & 0 \end{bmatrix}.$$

The entries of T' are nonnegative integers and T'_{ij} is the number of multiedges linking vertices α_i and β_j of G_{un} . Note that (1) G_{un} is an intersection multigraph whose family of sets are the polygons of the tessellations \mathcal{T}_1 and \mathcal{T}_2 , and (2) G_{un} is a root multigraph of G , that is, the line graph of G_{un} is G and there is a one-to-one correspondence between E_{un} and $V(G)$.

In order to find the eigenvectors of U_θ , we decompose the total state space as $\mathcal{H} = (\mathcal{A} + \mathcal{B}) \oplus (\mathcal{A} + \mathcal{B})^\perp$. In the next subsection, we address the subspace $\mathcal{A} \cap \mathcal{B} \subset \mathcal{A} + \mathcal{B}$, which is the one most amenable in terms of algebraic manipulations. In Subsection 4.2, we obtain the eigenvectors in subspace $(\mathcal{A} + \mathcal{B})$, and in Subsection 4.3 obtain the eigenvectors in subspace $(\mathcal{A} + \mathcal{B})^\perp = \mathcal{A}^\perp \cap \mathcal{B}^\perp$.

4.1 Space $\mathcal{A} \cap \mathcal{B}$

The following lemma shows a useful necessary and sufficient condition that the spectrum of T must obey in order to include eigenvalues ± 1 , which is important for obtaining the eigenvectors of U_θ . Besides, in the proof of this lemma, we describe a classical Markov chain induced by the quantum chain and how to obtain the classical detailed balance conditions from the quantum detailed balance conditions.

Lemma 4. *T is reversible with a reversible eigenfunction $\pi = \pi_1 \oplus \pi_2$ if and only if $\dim(\ker(I - T)) = \dim(\ker(I + T)) = 1$, $\ker(I - T) = \mathbb{C}(\pi_1 \oplus \pi_2)$, and $\ker(I + T) = \mathbb{C}(\pi_1 \oplus (-\pi_2))$.*

Proof. The following equivalences hold

$$\begin{aligned} f = f_1 \oplus f_2 \in \ker(I - T) &\Leftrightarrow T_{BA}f_1 = f_2, T_{AB}f_2 = f_1 \\ &\Leftrightarrow Af_1 = Bf_2 \\ &\Leftrightarrow a(u)f_1(\mathcal{T}_1(u)) = b(u)f_2(\mathcal{T}_2(u)), \end{aligned}$$

for any $u \in V$, which means that (a, b) obeys the QDB conditions and f is a reversible measure. The second equivalence is obtained as follows. If $T_{BA}f_1 = f_2$, $T_{AB}f_2 = f_1$, then $B^\dagger(Af_1 - Bf_2) = 0$, $A^\dagger(Af_1 - Bf_2) = 0$, which implies $Af_1 = Bf_2$; the opposite direction is obtained by taking B^\dagger and A^\dagger to both sides. Then,

$$\ker(I - T) = \{\pi \mid \pi \text{ is a reversible measure}\}.$$

Let us show that $\dim(\ker(I - T)) \leq 1$. Note that if T is nonreversible, then $\dim(\ker(I - T)) = 0$. Now we consider the reversible case and show $\dim(\ker(I - T)) = 1$.

By taking the square modulus of both sides of the QDB equation, and putting $p(e) := |a(e)|^2$ and $q(e) := |b(e)|^2$, we have $p(e)\zeta(\mathcal{T}_1(e)) = q(e)\zeta(\mathcal{T}_2(e))$ for every $e \in E(G_{\text{un}}) \simeq V(G)$, where $\zeta(\gamma) = |\pi(\gamma)|^2$ for $\gamma \in V(G_{\text{un}}) = \mathcal{T}_1 \sqcup \mathcal{T}_2$. Now we consider a classical Markov chain on G_{un} with the stochastic transition matrix P such that the transition probability from $\alpha \in \mathcal{T}_1$ to $\beta \in \mathcal{T}_2$ is

$$\langle \delta_\beta, P\delta_\alpha \rangle = \sum_{e: \mathcal{T}_1(e)=\alpha, \mathcal{T}_2(e)=\beta} p(e),$$

the transition probability from $\beta \in \mathcal{T}_2$ to $\alpha \in \mathcal{T}_1$ is

$$\langle \delta_\alpha, P\delta_\beta \rangle = \sum_{e: \mathcal{T}_1(e)=\alpha, \mathcal{T}_2(e)=\beta} q(e).$$

Note that the classical detailed balance conditions are

$$\langle \delta_\beta, P\delta_\alpha \rangle \zeta(\alpha) = \langle \delta_\alpha, P\delta_\beta \rangle \zeta(\beta).$$

By the Perron-Frobenius theorem, we have $\ker(I - P) = \mathbb{C}\zeta$. Besides, $T = \mathcal{M}^{-1}P\mathcal{M}$, where $(\mathcal{M}f)(\gamma) = \bar{\pi}(\gamma)f(\gamma)$, $\forall f \in \mathcal{K}$, and $\forall \gamma \in \mathcal{T}_1 \sqcup \mathcal{T}_2$. If there are two reversible eigenfunctions $\pi \neq \pi'$ of T , then $\pi'(\gamma) = e^{i\eta_\gamma}\pi(\gamma)$ for some $\eta_\gamma \in \mathbb{R}$. Then, by the definition of the QDB, we conclude that $\pi' = e^{i\eta_*}\pi$ for some constant $\eta_* \in \mathbb{C}$, and we obtain $\dim(\ker(I - T)) = 1$.

In general, by the property of the bipartiteness, $f_1 \oplus f_2 \in \ker(\mu - T)$ if and only if $f_1 \oplus (-f_2) \in \ker(\mu + T)$. We conclude that if T is reversible and $\pi_1 \oplus \pi_2$ is a reversible eigenfunction, then $\ker(I + T) = \mathbb{C}(\pi_1 \oplus (-\pi_2))$. \square

Corollary 2. T is nonreversible if and only if $\dim(\ker(I - T)) = \dim(\ker(I + T)) = 0$.

Recall that \mathcal{A} and \mathcal{B} are defined in Eqs. (2.4) and (2.5). If $\psi \in \mathcal{A} \cap \mathcal{B}$, then there exist $f \in \ell^2(\mathcal{T}_1)$ and $g \in \ell^2(\mathcal{T}_2)$ such that $\psi = Af = Bg$. This implies that $a(u)f(\mathcal{T}_1(u)) = b(u)g(\mathcal{T}_2(u))$ for every $u \in V$. By putting

$$\pi(\gamma) := \begin{cases} f(\gamma) & : \gamma \in \mathcal{T}_1, \\ g(\gamma) & : \gamma \in \mathcal{T}_2, \end{cases}$$

then $a(u)\pi(\mathcal{T}_1(u)) = b(u)\pi(\mathcal{T}_2(u))$ for every $u \in V$ and (a, b) obeys the QDB conditions and π is a reversible eigenfunction. If $f \oplus g$ is a reversible eigenfunction, then $f \oplus (-g) \in \ker(I + T)$.

Lemma 5. *The dimension of $\mathcal{A} \cap \mathcal{B}$ obeys*

$$\dim(\mathcal{A} \cap \mathcal{B}) \leq 1.$$

Moreover, $\dim(\mathcal{A} \cap \mathcal{B}) = 1$ if and only if T is reversible. The subspace $\mathcal{A} \cap \mathcal{B}$ is invariant under the action of U_θ whose eigenvalue is $-e^{2i\theta}$, and the eigenspace is described by

$$\mathcal{A} \cap \mathcal{B} = \mathbb{C}A\pi_1 = \mathbb{C}B\pi_2, \tag{4.8}$$

where $\pi_1 \oplus \pi_2$ is a reversible eigenfunction.

Proof. Let us prove the nontrivial part. If $\psi \in \mathcal{A} \cap \mathcal{B}$, then ψ is a $(e^{i\theta})$ -eigenvector of $e^{i\theta H_A}$ and $e^{i\theta H_B}$ because H_A and H_B are unitary and self-adjoint operators. Then, ψ is an eigenvector of U_θ with eigenvalue $(-e^{2i\theta})$. \square

These lemmas and corollary show that the reversibility of T plays an important role in the spectral analysis.

4.2 Space $\mathcal{A} + \mathcal{B}$ inherited from T

The next lemma shows that the action of U_θ on $\mathcal{A} + \mathcal{B}$ can be expressed in terms of T_{AB} and T_{BA} .

Lemma 6. *Let $L : \ell^2(\mathcal{T}_1) \oplus \ell^2(\mathcal{T}_2) \rightarrow \ell^2(V)$ be defined as $L(f \oplus g) = Af + Bg$ or, equivalently, $L = [A \ B]$. Then, we have*

$$U_\theta L = L\Lambda_\theta, \quad (4.9)$$

where

$$\Lambda_\theta = - \begin{bmatrix} I & 2ie^{-i\theta} \sin(\theta)T_{AB} \\ 2ie^{i\theta} \sin(\theta)T_{BA} & I - 4\sin^2(\theta)T_{BA}T_{AB} \end{bmatrix}. \quad (4.10)$$

Proof. The proof is obtained by employing Eqs. (2.7), property (2.6), the definitions of T_{AB} and T_{BA} , and by performing a straightforward calculation. \square

If $f \oplus g \in \ker(\lambda - \Lambda_\theta) \setminus \ker L$, then Lemma 6 implies that $Af + Bg \in \ker(\lambda - U_\theta) \setminus \{0\}$. This shows that the spectral decomposition of Λ_θ helps to obtain the spectral decomposition of U_θ . In the next subsection, we focus on the spectral decomposition of Λ_θ , and in the following one we address the kernel of L .

4.2.1 Spectral decomposition of Λ_θ

In Corollary 1, we have defined ϕ using equation $\cos \phi = \mu \sin \theta$, where μ is an eigenvalue of T and $\phi \in [0, \pi)$. Sometimes we denote ϕ by $\phi(\mu)$ to stress its relation with μ . The eigenspace of Λ_θ associated with the eigenvalue $e^{2i\phi(\mu)}$ is related with the eigenspace of T associated with eigenvalue μ as described by the following lemma.

Lemma 7. *Assume that $\theta \notin \{0, \pi\}$. Then,*

$$\ker(e^{2i\phi(\mu)} - \Lambda_\theta) = D \ker(\mu - T), \quad (4.11)$$

where D is the diagonal matrix defined by

$$D(f \oplus g) = f \oplus \left(ie^{i(\theta + \phi(\mu))} g \right).$$

Proof. After applying the Gaussian elimination method to $(e^{2i\phi} - \Lambda_\theta)$, we obtain

$$\ker(e^{2i\phi} - \Lambda_\theta) = \ker \left(\frac{\cos \phi}{\sin \theta} - DTD^{-1} \right).$$

As a last step we use the fact that $\ker(\mu - DTD^{-1}) = D \ker(\mu - T)$. \square

The last lemma shows that the spectrum of Λ_θ can be obtained from the spectrum of T , that is, $e^{2i\phi}$ can be obtained from μ using $\cos \phi = \mu \sin \theta$. Now we list some relevant observations about the eigenvalues of Λ_θ (see Fig. 1).

- (1) There is a spectral gap if $\theta \neq \pi/2$. In fact, $\sigma(\Lambda_\theta) \subset \{e^{2i\phi} \mid \cos 2\phi \in [-1, \cos(\pi - 2\theta)]\}$ because $\cos 2\phi = 2\mu^2 \sin^2 \theta - 1$ and $|\mu| \leq 1$.
- (2) Map ϕ is a bijection if $\theta \neq \pi/2$. In fact, all eigenvalues of Λ_θ are inherited from eigenvalues of T and there is a one-to-one correspondence between $\sigma(\Lambda_\theta)$ and $\sigma(T)$. On the other hand, if $\theta = \pi/2$, the spectral gap disappears. In this case, if T has a quantum detailed balance, ϕ is not a bijection because $\phi(1) = \phi(-1) = 0$.
- (3) The spectrum of Λ_θ is symmetric. In fact, $e^{2i\phi} \in \sigma(\Lambda_\theta)$ if and only if $e^{2i(\pi - \phi)} = e^{-2i\phi} \in \sigma(\Lambda_\theta)$ because there is an equivalence between “ $\mu \in \sigma(T)$ with $f \oplus g \in \ker(\mu - T)$ ” and “ $-\mu \in \sigma(T)$ with $f \oplus (-g) \in \ker(\mu + T)$ ” since G_{un} is bipartite.

4.2.2 Kernel of L

From now on, to obtain an eigenfunction of U_θ restricted to the subspace $\mathcal{A} + \mathcal{B}$, we use a lift-up operation LD from the set of the eigenfunctions of Λ_θ in $\ell^2(\mathcal{T}_1) \oplus \ell^2(\mathcal{T}_2)$ to the original space $\ell^2(V)$. Recall that the eigenfunctions of Λ_θ should not be in the kernel of L . It is therefore natural to characterize the kernel of L .

Lemma 8.

$$\ker(L) = \ker(I + T) = \ker(e^{-2i\theta} + \Lambda_\theta)$$

Proof. If $f \oplus g \in \ker L$, then $Af + Bg = 0$ which implies that $f + T_{AB}g = 0$ and $g + T_{BA}f = 0$ after left-multiplying by A^\dagger and B^\dagger , respectively. Then, $f \oplus g \in \ker(I + T)$. On the other hand, if $f \oplus g \in \ker(I + T)$, then $f + T_{AB}g = 0$ and $g + T_{BA}f = 0$, which implies that $A^\dagger(Af + Bg) = 0$ and $B^\dagger(Af + Bg) = 0$. Then, $Af + Bg$ must be 0, or equivalently, $f \oplus g \in \ker L$. We conclude that $\ker L = \ker(I + T)$.

The second equality $\ker(I + T) = \ker(e^{-2i\theta} + \Lambda_\theta)$ is obtained by applying the Gaussian elimination method to $(e^{-2i\theta} + \Lambda_\theta)$. \square

Let us make a useful characterization of the eigenspace described by $\ker(\lambda - U|_{\mathcal{A} + \mathcal{B}})$. From Lemmas 6 and 8, it follows that

$$\ker((\lambda - U_\theta)L) = \ker((I + T)(\lambda - \Lambda_\theta)) = \ker\left((e^{-2i\theta} + \Lambda_\theta)(\lambda - \Lambda_\theta)\right). \quad (4.12)$$

Consider the nonreversible case. Corollary 2 states that in this case $\ker(I + T) = \{0\}$, that is, $I + T$ is invertible and Eq. (4.12) can be further reduced to

$$\ker\left((e^{2i\phi} - U_\theta)L\right) = \ker\left(e^{2i\phi} - \Lambda_\theta\right) = D \ker\left(\frac{\cos \phi}{\sin \theta} - T\right).$$

Then, when T is nonreversible, all eigenvalues of U_θ associated with the invariant subspace $\mathcal{A} + \mathcal{B}$ are obtained from the eigenvalues of T .

Consider the reversible case. By (4.12) and Lemma 8, if $e^{2i\phi} \neq -e^{-2i\theta}$, then

$$\ker\left((e^{2i\phi} - U_\theta)L\right) \setminus \ker L = \ker\left(e^{2i\phi} - \Lambda_\theta\right) = D \ker\left(\frac{\cos \phi}{\sin \theta} - T\right). \quad (4.13)$$

Note that we obtain the eigenvalues of U_θ associated only with eigenvectors that do not belong to the kernel of L . Now we analyze the boundaries of the spectrum of Λ_θ , which are $2\phi_+ := \pi - 2\theta$ and $2\phi_- := \pi + 2\theta$. These boundaries exist only if $\theta \neq \pi/2$ as can be seen in Fig. 1. Still in the reversible case, we split the analysis into two cases.

Case $\theta \neq \pi/2$. Counting the dimension of $\mathcal{A} + \mathcal{B}$ inherited from the eigenspace of Λ_θ except the eigenspace with the eigenvalue $e^{2i\phi_+}$, we have

$$\begin{aligned} \sum_{\phi \neq \phi_+} \dim \ker\left(e^{2i\phi} - U_\theta|_{\mathcal{A} + \mathcal{B}}\right) &= \sum_{\phi \neq \phi_+} \dim\left(D \ker\left(\frac{\cos \phi}{\sin \theta} - T\right)\right) \\ &= |V_{\text{un}}| - \dim \ker(I - T) \\ &= |V_{\text{un}}| - 1. \end{aligned}$$

On the other hand, since T is reversible, then $\dim(\mathcal{A} + \mathcal{B})^\perp = b_1(G_{\text{un}}) = |E_{\text{un}}| - |V_{\text{un}}| + 1$ by (4.16). If $e^{2i\phi_+} \in \sigma(U_\theta|_{\mathcal{A} + \mathcal{B}})$, then $\sum_\lambda \dim(\ker(\lambda - U_\theta)) > |E_{\text{un}}| = |V(G)|$, which is a contradiction. Then, $e^{2i\phi_+} \notin \sigma(U_\theta|_{\mathcal{A} + \mathcal{B}})$.

Case $\theta = \pi/2$. Eq. (4.13) and the same results of the case $\theta \neq \pi/2$ hold in the present case, unless $\phi = 0$, which implies that $\theta = \pi/2$. When $\phi = 0$, we have

$$\ker((I - U_{\pi/2})L) = \ker((I - \Lambda_{\pi/2})^2) = \ker((I - T)(I + T)) = \ker(I - T) \oplus \ker L. \quad (4.14)$$

The third expression is obtained by a Gaussian elimination and the final expression comes from Lemma 8. Using Lemma 5, we obtain $\ker(I - U_{\pi/2}|_{\mathcal{A}+\mathcal{B}}) = L \ker(I - T) = \mathbb{C} A\pi_1$.

Now we summarize the statements related to $\ker(\lambda - U|_{\mathcal{A}+\mathcal{B}})$:

(1) Non-reversible case:

$$\ker(e^{2i\phi} - U|_{\mathcal{A}+\mathcal{B}}) = LD \ker\left(\frac{\cos \phi}{\sin \theta} - T\right)$$

(2) Reversible case:

(a) If $\theta \neq \pi/2$, then

$$\ker(e^{2i\phi} - U|_{\mathcal{A}+\mathcal{B}}) = \begin{cases} LD \ker\left(\frac{\cos \phi}{\sin \theta} - T\right) & \text{if } \phi \neq \phi_+, \\ 0 & \text{if } \phi = \phi_+. \end{cases}$$

(b) If $\theta = \pi/2$, then

$$\ker(e^{2i\phi} - U|_{\mathcal{A}+\mathcal{B}}) = \begin{cases} LD \ker(\cos \phi - T) & \text{if } \phi \neq 0, \\ \mathbb{C} A\pi_1 & \text{if } \phi = 0. \end{cases}$$

4.3 Cycle-path space $(\mathcal{A} + \mathcal{B})^\perp$

In this subsection we address the subspace $\mathcal{A}^\perp \cap \mathcal{B}^\perp$, the dimension of which depends on the reversibility of T . Using

$$\dim(\mathcal{A} + \mathcal{B}) = \dim(\mathcal{A}) + \dim(\mathcal{B}) - \dim(\mathcal{A} \cap \mathcal{B})$$

and Lemma 5, we have

$$\dim(\mathcal{A}^\perp \cap \mathcal{B}^\perp) = \begin{cases} \nu - m - n + 1 & \text{if } T \text{ is reversible,} \\ \nu - m - n & \text{otherwise.} \end{cases} \quad (4.15)$$

The dimension is expressed by the first Betti number $b_1(G_{\text{un}})$ of the underlying bipartite multi-graph G_{un} , that is,

$$\dim(\mathcal{A}^\perp \cap \mathcal{B}^\perp) = \begin{cases} b_1(G_{\text{un}}) & \text{if } T \text{ is reversible,} \\ b_1(G_{\text{un}}) - 1 & \text{otherwise,} \end{cases} \quad (4.16)$$

because the number of edges of G_{un} is ν (G is the line graph of G_{un}), the number of vertices of G_{un} is $|\mathcal{T}_1| + |\mathcal{T}_2| = m + n$, and by definition $b_1(G_{\text{un}}) = |E_{\text{un}}| - |V_{\text{un}}| + 1$. In fact, the first Betti number is equal to the number of fundamental cycles. Here a fundamental cycle is the cycle generated by adding one edge of the original graph to the spanning tree. Since there is a one-to-one correspondence between the set of fundamental cycles and the set of edges

not in the spanning tree, $b_1(G_{\text{un}})$ is equal to the number of edges of G_{un} not in the spanning tree. The number of edges in the spanning tree of G_{un} is $|V(G_{\text{un}})| - 1 = m + n - 1$. Then, $b_1(G_{\text{un}}) = \nu - m - n + 1$.

Let Γ_{un} be a set of fundamental cycles of G_{un} . In the reversible case, there is a one-to-one correspondence between Γ_{un} and a basis of the vector space $\mathcal{A}^\perp \cap \mathcal{B}^\perp$, which is isomorphic to the cycle space [8]. In Proposition 1, we show how to obtain an eigenvector of U_θ with eigenvalue $(-e^{-2i\theta})$ associated with a fundamental cycle. In the nonreversible case, we have to fix one fundamental cycle and choose a second fundamental cycle and then we link these cycles with a path when they have no overlap forming a cycle-path subgraph. Since one cycle in Γ_{un} remains fixed, this explains why there is a (-1) in Eq. (4.16) in the nonreversible case. The vector space $\mathcal{A}^\perp \cap \mathcal{B}^\perp$ is not isomorphic to the cycle space. In Proposition 2, we show how to obtain an eigenvector of U_θ with eigenvalue $(-e^{-2i\theta})$ associated with the cycle-path subgraph.

Lemma 9. *If $\psi \in \mathcal{A}^\perp \cap \mathcal{B}^\perp$, then ψ is an eigenfunction of U_θ with eigenvalue $(-e^{-2i\theta})$.*

Proof. If $\psi \in \mathcal{A}^\perp \cap \mathcal{B}^\perp$, then ψ is a $(e^{-i\theta})$ -eigenvector of $e^{i\theta H_A}$ and $e^{i\theta H_B}$ because H_A and H_B are unitary and self-adjoint operators. Then, ψ is an eigenfunction of $U_\theta (= -e^{i\theta H_B} e^{i\theta H_A})$ with eigenvalue $(-e^{-2i\theta})$. \square

Since G is the line graph of G_{un} , there is a bijection map $\eta : E_{\text{un}} \rightarrow V(G)$, which we use in the following propositions.

Proposition 1. *Suppose that T is reversible. Then, for each $c \in \Gamma_{\text{un}}$, there is an eigenfunction ψ_c in $\mathcal{A}^\perp \cap \mathcal{B}^\perp$ whose support is $\text{supp}(\psi_c) = \{\eta(e) \mid e \in E(c)\}$. Moreover,*

$$\mathcal{A}^\perp \cap \mathcal{B}^\perp = \ker \left(e^{-2i\theta} + U_\theta|_{\mathcal{A}^\perp \cap \mathcal{B}^\perp} \right) = \text{span}\{\psi_c \mid c \in \Gamma_{\text{un}}\}. \quad (4.17)$$

Proof. Define $\mathcal{U}_\eta : \ell^2(E_{\text{un}}) \rightarrow \ell^2(V(G))$ so that $\mathcal{U}_\eta(\psi)(u) = \psi(\eta^{-1}(u))$. Note that $\mathcal{U}_\eta(\psi) \in \mathcal{A}^\perp$ if and only if

$$\sum_{e: \mathcal{T}_1(\eta(e))=\alpha} \bar{a}(\eta(e)) \psi(e) = 0 \quad (4.18)$$

for $\alpha \in \mathcal{T}_1$, where the sum runs over the edges incident to $\alpha \in \mathcal{T}_1$ in G_{un} and $\bar{a}(\eta(e))$ is the complex conjugate of $a(\eta(e))$. $\mathcal{U}_\eta(\psi) \in \mathcal{B}^\perp$ if and only if

$$\sum_{e: \mathcal{T}_2(\eta(e))=\beta} \bar{b}(\eta(e)) \psi(e) = 0 \quad (4.19)$$

for $\beta \in \mathcal{T}_2$, where the sum runs over the edges incident to $\beta \in \mathcal{T}_2$ in G_{un} . We use Eqs. (4.18) and (4.19) to obtain the entries of an eigenfunction with support on a fundamental cycle. From now on, we consider space $\ell^2(E_{\text{un}})$, which is lifted to $\ell^2(V(G))$ by the unitary map \mathcal{U}_η . For the sake of simplicity, we denote $a(\eta(e))$ by $a(e)$ and $b(\eta(e))$ by $b(e)$ for $e \in E_{\text{un}}$.

Let $c \in \Gamma_{\text{un}}$. Since G_{un} is a bipartite multigraph, c is an even cycle. In the following, we describe an important property of a reversible measure on V_{un} using this cycle and then we construct an eigenfunction $\psi_c \in \ell^2(E_{\text{un}})$ so that $\mathcal{U}_\eta(\psi_c) \in \mathcal{A}^\perp \cap \mathcal{B}^\perp$ and whose support is $E(c) = \{e_1, e_2, \dots, e_{2k}\}$. The vertices are labeled by $u_1 = e_1 \cap e_2, u_2 = e_2 \cap e_3, \dots, u_{2k} = e_{2k} \cap e_1$ and $u_{2j} \in \mathcal{T}_1$ and $u_{2j-1} \in \mathcal{T}_2$ for $j = 1, \dots, k$.

Since T is reversible, there is a reversible measure π on V_{un} . Redefining π so that $\pi(u_{2k}) = 1$ and considering the vertices u_{2k} and u_1 connected by the edge e_1 , the quantum detailed balance equation of Def. 2 implies that $a(e_1)\pi(u_{2k}) = b(e_1)\pi(u_1)$, which simplifies to $\pi(u_1) =$

$a(e_1)/b(e_1)$. Now we consider the neighboring vertices u_1 and u_2 connected by the edge e_2 . We have $b(e_2)\pi(u_1) = a(e_2)\pi(u_2)$, which simplifies to $\pi(u_2) = b(e_2)a(e_1)/a(e_2)b(e_1)$. We proceed systematically considering the edges of the cycle c until the final edge e_{2k} , which must satisfy

$$\frac{b(e_{2k})a(e_{2k-1}) \cdots b(e_2)a(e_1)}{a(e_{2k})b(e_{2k-1}) \cdots a(e_2)b(e_1)} = \pi(u_{2k}) = 1. \quad (4.20)$$

Now we describe the procedure that generates the eigenfunction $\mathcal{U}_\eta(\psi_c) \in \mathcal{A}^\perp \cap \mathcal{B}^\perp$ so that $\text{supp}(\psi_c) = E(c)$. Setting $\psi_c(e_1) = 1$ and considering the edges e_1 and e_2 with the common vertex u_1 , Eq. (4.19) implies that $\bar{b}(e_1)\psi_c(e_1) + \bar{b}(e_2)\psi_c(e_2) = 0$ because $\mathcal{U}_\eta(\psi_c) \in \mathcal{B}^\perp$, which simplifies to $\psi_c(e_2) = -\bar{b}(e_1)/\bar{b}(e_2)$. Next, since $\mathcal{U}_\eta(\psi_c) \in \mathcal{A}^\perp$, considering the edges e_2 and e_3 with the common vertex u_2 , Eq. (4.18) implies that $\bar{a}(e_2)\psi_c(e_2) + \bar{a}(e_3)\psi_c(e_3) = 0$, which simplifies to $\psi_c(e_3) = \bar{a}(e_2)\bar{b}(e_1)/\bar{a}(e_3)\bar{b}(e_2)$. We proceed systematically until the final vertex u_{2k} . Then, we close the cycle with no conflict because if we take one step further, we use (4.20) and we obtain the consistency equation

$$\frac{\bar{a}(e_{2k})\bar{b}(e_{2k-1}) \cdots \bar{a}(e_2)\bar{b}(e_1)}{\bar{a}(e_1)\bar{b}(e_{2k}) \cdots \bar{a}(e_3)\bar{b}(e_2)} = \psi_c(e_1) = 1.$$

Summing up, the even entries of the eigenfunction are

$$\psi_c(e_{2j}) = -\frac{\bar{b}(e_{2j-1}) \cdots \bar{a}(e_2)\bar{b}(e_1)}{\bar{b}(e_{2j}) \cdots \bar{a}(e_3)\bar{b}(e_2)}, \quad (4.21)$$

and the odd entries of the eigenfunction are

$$\psi_c(e_{2j+1}) = \frac{\bar{a}(e_{2j})\bar{b}(e_{2j-1}) \cdots \bar{a}(e_2)\bar{b}(e_1)}{\bar{a}(e_{2j+1})\bar{b}(e_{2j}) \cdots \bar{a}(e_3)\bar{b}(e_2)}. \quad (4.22)$$

Note that by construction $\mathcal{U}_\eta(\psi_c) \in \mathcal{A}^\perp \cap \mathcal{B}^\perp$ and $\text{supp}(\mathcal{U}_\eta(\psi_c)) = \{\eta(e) \mid e \in E(c)\}$. Using Lemma 9, we conclude that the above procedure generates a linearly independent eigenfunction with eigenvalue $(-e^{-2i\theta})$ for each fundamental cycle. Since the number of fundamental cycles is equal to $\dim(\mathcal{A}^\perp \cap \mathcal{B}^\perp)$ in the reversible case, the set of the eigenfunctions $\mathcal{U}_\eta(\psi_c)$ is an eigenbasis of $\mathcal{A}^\perp \cap \mathcal{B}^\perp$. \square

In the nonreversible case, we need to construct a graph using two fundamental cycles.

Construction 1. Let c_0 and c be fundamental cycles. Define graph $G_c^{c_0}$, subgraph of G_{un} , obeying the following rules: (1) If $V(c_0) \cap V(c) \neq \emptyset$, then $G_c^{c_0} = (V(c_0) \cup V(c), E(c_0) \cup E(c))$, that is, $G_c^{c_0}$ is the union of c_0 and c , and (2) if $V(c_0) \cap V(c) = \emptyset$, then $G_c^{c_0}$ is the union of c_0 , c , and a path p connecting c_0 and c so that $E(p) \cap (E(c_0) \cup E(c)) = \emptyset$.

Proposition 2. Suppose that T is nonreversible. Let c_0 and c be cycles in Γ_{un} and let $G_c^{c_0}$ be a graph obtained from Construction 1. Then, for each $c \in \Gamma_{\text{un}} \setminus \{c_0\}$, there is an eigenfunction $\psi_c^{c_0}$ in $\mathcal{A}^\perp \cap \mathcal{B}^\perp$ whose support is $\text{supp}(\psi_c^{c_0}) = \{\eta(e) \mid e \in E(G_c^{c_0})\}$. Moreover,

$$\mathcal{A}^\perp \cap \mathcal{B}^\perp = \ker \left(e^{-2i\theta} + U_\theta|_{\mathcal{A}^\perp \cap \mathcal{B}^\perp} \right) = \text{span}\{\psi_c^{c_0} \mid c \in \Gamma_{\text{un}} \setminus \{c_0\}\}. \quad (4.23)$$

Proof. Let c_0 and c be fundamental cycles. The vertices of c_0 and c are labeled by $\{x_1, \dots, x_{2k}\}$ and $\{y_1, \dots, y_{2k'}\}$, respectively, and the edges of c_0 are $e_1 = \{x_{2k}, x_1\}$, $e_2 = \{x_1, x_2\}, \dots, e_{2k} = \{x_{2k-1}, x_{2k}\}$, and the edges of c are $f_1 = \{y_{2k'}, y_1\}$, $f_2 = \{y_1, y_2\}, \dots, f_{2k'} = \{y_{2k'-1}, y_{2k'}\}$, where $x_{2j} \in \mathcal{T}_1$ and $x_{2j-1} \in \mathcal{T}_2$. Let \mathcal{U}_η be the operator defined in the proof of Proposition 1.

Case 1. Suppose that $V(c_0) \cap V(c) = \emptyset$. Then, there is a path p connecting the two cycles from $x_{2k} \in V(c_0)$ to $y_{2k'} \in V(c)$. Denote the vertices of the path by $\{x_{2k} = z_1, z_2, \dots, z_{\ell+1} = y_{2k'}\}$ and the edges by $g_1 = \{z_1, z_2\}, g_2 = \{z_2, z_3\}, \dots, g_\ell = \{z_\ell, z_{\ell+1}\}$.

Now we construct function $\psi_c^{c_0}$ whose support is $E(G_c^{c_0})$. Let us define balancing indices $\Delta(c_0)$ and $\Delta(c)$ for cycles c_0 and c , so that

$$\begin{aligned}\Delta(c_0) &= \frac{a(e_{2k})b(e_{2k-1}) \cdots a(e_2)b(e_1)}{b(e_{2k})a(e_{2k-1}) \cdots b(e_2)a(e_1)} - 1, \\ \Delta(c) &= \frac{a(f_{2k'})b(f_{2k'-1}) \cdots a(f_2)b(f_1)}{b(f_{2k'})a(f_{2k'-1}) \cdots b(f_2)a(f_1)} - 1.\end{aligned}$$

Note that in the reversible case we would have $\Delta(c_0) = \Delta(c) = 0$. Since we are addressing the nonreversible case, we do have $\Delta(c_0) = \Delta(c) \neq 0$. Using the same procedure of Proposition 1, we start from vertex x_1 with $\psi_c^{c_0}(e_1) = 1$ and proceed until x_{2k-1} . The entries of $\psi_c^{c_0}$ on c_0 are given by Eqs. (4.21) and (4.22).

The last vertex x_{2k} has three incident edges in $G_c^{c_0}$ and Eq. (4.18) implies that $\bar{a}(e_1)\psi_c^{c_0}(e_1) + \bar{a}(e_{2k})\psi_c^{c_0}(e_{2k}) + \bar{a}(g_1)\psi_c^{c_0}(g_1) = 0$ because $\mathcal{U}_\eta(\psi_c^{c_0}) \in \mathcal{A}^\perp$. Using the expression of $\psi_c^{c_0}(e_{2k})$ and the balancing index $\Delta(c_0)$, we obtain

$$\bar{\psi}_c^{c_0}(g_1) = \frac{a(e_1)}{a(g_1)}\Delta(c_0). \quad (4.24)$$

Continuing to use the procedure from z_2 going along the path p until z_ℓ , we obtain

$$\bar{\psi}_c^{c_0}(g_\ell) = \begin{cases} -\frac{\kappa(p)a(e_1)\Delta(c_0)}{a(g_\ell)} & \text{if } \ell \text{ is even,} \\ +\frac{\kappa(p)a(e_1)\Delta(c_0)}{b(g_\ell)} & \text{if } \ell \text{ is odd,} \end{cases} \quad (4.25)$$

where

$$\kappa(p) = \begin{cases} \frac{a(g_\ell)b(g_{\ell-1}) \cdots a(g_2)b(g_1)}{b(g_\ell)a(g_{\ell-1}) \cdots b(g_2)a(g_1)} & \text{if } \ell \text{ is even,} \\ \frac{b(g_\ell)a(g_{\ell-1}) \cdots a(g_2)b(g_1)}{a(g_\ell)b(g_{\ell-1}) \cdots b(g_2)a(g_1)} & \text{if } \ell \text{ is odd.} \end{cases}$$

Now we restart the procedure in order to find the entries of $\psi_c^{c_0}$ on the cycle c . We start from y_1 with an arbitrary $\psi_c^{c_0}(f_1)$ and proceed until $y_{2k'-1}$. The goal is to obtain $\psi_c^{c_0}(f_1)$ that consistently closes the process. Suppose that the length ℓ of path p is even. Then, $y_{2j} \in \mathcal{T}_1$ and $y_{2j-1} \in \mathcal{T}_2$. In this case, the tessellations of cycles c_0 and c are symmetric and we can use the result of Eq. (4.24) by replacing g_1 by g_ℓ and edges e by edges f , that is,

$$\bar{\psi}_c^{c_0}(g_\ell) = \frac{a(f_1)}{a(g_\ell)}\Delta(c)\bar{\psi}_c^{c_0}(f_1). \quad (4.26)$$

In order to obtain a consistent result, we use Eq. (4.25) (even ℓ) to determine $\bar{\psi}_c^{c_0}(f_1)$, which is the only one missing. The result is

$$\bar{\psi}_c^{c_0}(f_1) = -\kappa(p)\frac{a(e_1)\Delta(c_0)}{a(f_1)\Delta(c)}. \quad (4.27)$$

Suppose that the length of path p is odd, where the length is the number of edges. Then, $y_{2j-1} \in \mathcal{T}_1$ and $y_{2j} \in \mathcal{T}_2$. In this case, the tessellations of cycles c_0 and c are antisymmetric and we have to recalculate Eq. (4.26). The new result is

$$\bar{\psi}_c^{c_0}(g_\ell) = \frac{b(f_1)}{b(g_\ell)}\tilde{\Delta}(c)\bar{\psi}_c^{c_0}(f_1),$$

where $\tilde{\Delta}(c)$ is obtained from $\Delta(c)$ by interchanging a and b . Again, in order to obtain a consistent result, we use Eq. (4.25) (odd ℓ) to determine the $\bar{\psi}_c^{c_0}(f_1)$. The result is

$$\bar{\psi}_c^{c_0}(f_1) = \kappa(p) \frac{a(e_1)\Delta(c_0)}{b(f_1)\tilde{\Delta}(c)}. \quad (4.28)$$

By construction $\mathcal{U}_\eta(\psi_c^{c_0}) \in \mathcal{A}^\perp \cap \mathcal{B}^\perp$ and $\text{supp}(\psi_c^{c_0}) = E(G_c^{c_0})$.

Case 2. Suppose that $V(c_0) \cap V(c) \neq \emptyset$. In this case, the intersection of the two fundamental cycles of $G_c^{c_0}$ is either a vertex or a path [12]. The path length is odd if $|V(c_0) \cap V(c)|$ is even and the path length is even if $|V(c_0) \cap V(c)|$ is odd. In both situations, we start with the cycle c_0 using the same procedure of Case 1, but this time there are two degree-3 vertices (or one degree-4 if $|V(c_0) \cap V(c)| = 1$). As before, we assume that $\psi^{c_0}(e_1) = 1$ and proceed along the edges of c_0 . Then, we restart the procedure with cycle c with arbitrary $\psi_c(f_1)$ and proceed along c . The entries of ψ^{c_0} on c_0 are given by Eqs. (4.21) and (4.22) and the entries of ψ_c on c are given by Eqs. (4.21) and (4.22) after multiplying the right-hand side by $\psi_c(f_1)$ and after interchanging e_{2j} and e_{2j+1} by f_{2j} and f_{2j+1} , respectively. There is an identification of edges of c_0 and c along the path. The eigenvector with support on the union of the cycles is $\psi_c^{c_0} = \psi^{c_0} + \psi_c$. In order to close the set of all equations based on Eqs. (4.18) and (4.19), we have to set

$$\bar{\psi}_c(f_1) = -\frac{a(e_1)\Delta(c_0)}{a(f_1)\Delta(c)}, \quad (4.29)$$

which is the same as the one given by Eq. (4.27) if we take $\kappa(p) = 1$.

Note that by construction $\mathcal{U}_\eta(\psi_c^{c_0}) \in \mathcal{A}^\perp \cap \mathcal{B}^\perp$ and $\text{supp}(\mathcal{U}_\eta(\psi_c^{c_0})) = \{\eta(e) \mid e \in E(G_c^{c_0})\}$. Using Lemma 9, we conclude that the above procedure generates a linearly independent eigenfunction with eigenvalue $(-e^{-2i\theta})$ for each fundamental cycle $c \in \Gamma_{\text{un}} \setminus \{c_0\}$. Since the number of fundamental cycles in $\Gamma_{\text{un}} \setminus \{c_0\}$ is equal to $\dim(\mathcal{A}^\perp \cap \mathcal{B}^\perp)$ in the nonreversible case, the set of the eigenfunctions $\mathcal{U}_\eta(\psi_c^{c_0})$ is an eigenbasis of $\mathcal{A}^\perp \cap \mathcal{B}^\perp$. \square

5 Main theorem

Suppose we have defined a 2-tessellable quantum walk as described in Section 2. We also assume that the quantities and the notations of Secs. 3 and 4 are known. For instance, ϕ and ϕ_\pm are defined as $\cos \phi(\mu) = \mu \sin \theta$ and $\phi_\pm = \pi/2 \mp \theta$. We summarize our results in the following theorem.

Theorem 2. U_θ can be decomposed into $U_\theta|_{\mathcal{A}+\mathcal{B}} \oplus U_\theta|_{(\mathcal{A}+\mathcal{B})^\perp}$ under the decomposition of $\mathcal{H} = (\mathcal{A} + \mathcal{B}) \oplus (\mathcal{A} + \mathcal{B})^\perp$. Each invariant space is further decomposed as follows.

(1) Space $\mathcal{A} + \mathcal{B}$.

$$\sigma(U_\theta|_{\mathcal{A}+\mathcal{B}}) = \begin{cases} \{e^{2i\phi(\mu)} \mid \mu \in \sigma(T)\} & \text{if } T \text{ is nonreversible,} \\ \{e^{2i\phi(\mu)} \mid \mu \in \sigma(T) \setminus \{1\}\} & \text{if } T \text{ is reversible and } \theta \neq \pi/2, \\ \{e^{2i\phi(\mu)} \mid \mu \in \sigma(T) \setminus \{-1\}\} & \text{if } T \text{ is reversible and } \theta = \pi/2. \end{cases}$$

$$\ker(U_\theta|_{\mathcal{A}+\mathcal{B}} - e^{2i\phi}) = \begin{cases} \left\{ Af + ie^{i(\theta+\phi)}Bg \mid f \oplus g \in \ker\left(\frac{\cos\phi}{\sin\theta} - T\right) \right\} & \text{if } \phi \neq \phi_-, \\ \mathcal{A} \cap \mathcal{B} = \mathbb{C}A\pi_1 & \text{if } \phi = \phi_- \text{ and } T \text{ is reversible,} \\ 0 & \text{if } \phi = \phi_- \text{ and } T \text{ is nonreversible,} \end{cases}$$

where $\pi_1 \oplus \pi_2 \in \ker(1 - T)$, which is a reversible measure of T .

(2) Space $(\mathcal{A} + \mathcal{B})^\perp$.

$$\sigma(U_\theta|_{(\mathcal{A}+\mathcal{B})^\perp}) = \begin{cases} \emptyset & \text{if } G_{un} \text{ is a tree or } "b(G_{un}) = 1 \text{ and } T \text{ is nonreversible",} \\ -e^{-2i\theta} & \text{otherwise.} \end{cases}$$

$$\ker(U_\theta|_{(\mathcal{A}+\mathcal{B})^\perp} + e^{-2i\theta}) = \begin{cases} \text{span}\{\psi_c \mid c \in \Gamma(G_{un})\} & \text{if } T \text{ is reversible,} \\ \text{span}\{\psi_c^{c_0} \mid c \in \Gamma(G_{un}) \setminus \{c_0\}\} & \text{otherwise.} \end{cases}$$

If T is reversible, then the dimension of $(\mathcal{A} + \mathcal{B})^\perp$ is $\nu - (m+n) + 1$, otherwise, $\nu - (m+n)$.

Note that the eigenvalues of U_θ were obtained via two different methods. The first method is described in Section 3 and the eigenvalues are listed in Corollary 1, items (1) and (2). The second method is described in Section 4 and were obtained using Gaussian elimination method. Note that those methods are consistent with each other.

6 Example: kagome lattice

The kagome (or trihexagonal) lattice [28, 25, 16] is known to be the line graph of the hexagonal lattice and it is straightforward to check that the hexagonal lattice is the clique graph of the kagome lattice. The kagome lattice is 2-tessellable because the hexagonal lattice is 2-colorable, as can be checked in Fig. 2(a). Fig. 2(a) also shows how we have embedded the kagome lattice in \mathbb{R}^2 . For each horizontal line, there are upper and lower triangles at each crossing with a vertical line. Take the lower red triangle in the center of Fig. 2(a), whose vertices are labeled by $\{1, 2, 3\}$, as a representative cell at $(x, y) \in \mathbb{Z}^2$. Then, each vertex of the kagome lattice is represented by $\mathbb{Z}^2 \times \{1, 2, 3\}$. Fig. 2(b) shows the underlying graph, which is the hexagonal lattice.

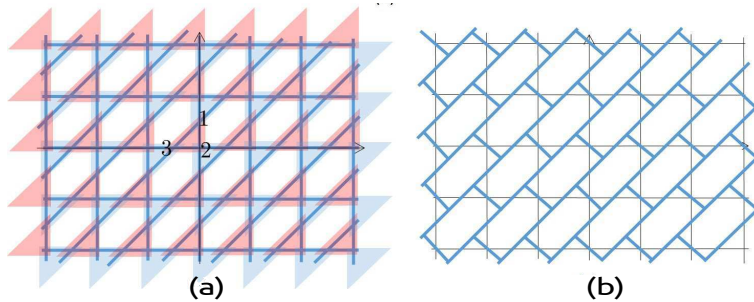


Figure 2: Graph (a) depicts the embedding of the kagome lattice and a tessellation cover, where \mathcal{T}_1 is comprised the red tiles and \mathcal{T}_2 the blue tiles. Note the labeling of the red clique in the center. Graph (b) describes the underlying bipartite graph, which is the hexagonal lattice.

Let \mathcal{T}_1 and \mathcal{T}_2 be the tessellations comprising the upper triangles and the lower triangles, respectively. Define the 3-dimensional self-adjoint unitary operators associated with each clique $E_1 = 2|\alpha\rangle\langle\alpha| - 1$ and $E_2 = 2|\beta\rangle\langle\beta| - 1$, where $|\alpha\rangle$ and $|\beta\rangle$ are unit vectors in \mathbb{C}^3 . Set $H_1 := \bigoplus_{\mathcal{T}_1} E_1$ and $H_2 := \bigoplus_{\mathcal{T}_2} E_2$. Then, the evolution operator is $U_\theta = -e^{i\theta H_2} e^{i\theta H_1}$.

Due to the translational symmetries of the kagome lattice, we can use the Fourier transform $\mathcal{F} : \ell^2(\mathbb{Z}^2 \times \{1, 2, 3\}) \rightarrow L^2([0, 2\pi]^2 \times \{1, 2, 3\})$, which is defined by

$$\hat{\psi}(k, l, j) := (\mathcal{F}\psi)(k, l, j) = \sum_{x, y \in \mathbb{Z}} \psi(x, y, j) e^{i(kx + ly)},$$

where $j \in \{1, 2, 3\}$, and its inverse by

$$\psi(x, y, j) := (\mathcal{F}^{-1}\hat{\psi})(x, y, j) = \frac{1}{(2\pi)^2} \int_0^{2\pi} \int_0^{2\pi} \hat{\psi}(k, l, j) e^{-i(kx + ly)} dk dl.$$

In the Fourier space, the dynamic is described by a reduced 3×3 evolution operator

$$\hat{U}_\theta(k, l) := -W_{k,l} e^{i\theta E_2} W_{k,l}^\dagger e^{i\theta E_1} = -e^{i\theta E'_2(k,l)} e^{i\theta E_1}, \quad (6.30)$$

where $W_{k,l} = \text{diag}(1, e^{il}, e^{i(k+l)})$ and $E'_2(k, l) = 2|\beta'(k, l)\rangle\langle\beta'(k, l)| - 1$ with $|\beta'(k, l)\rangle = W_{k,l}|\beta\rangle$, which can be obtained directly from the quotient graph of the kagome lattice (see left-hand graph of Fig. 3). A tessellation cover of the quotient graph comprises two polygons, which are associated with vectors $|\alpha\rangle$ and $|\beta'(k, l)\rangle$. The intersection graph of the quotient graph is the right-hand graph of Fig. 3. The discriminant operator of $\hat{U}_\theta(k, l)$ for $|\alpha\rangle = |\beta\rangle = 1/\sqrt{3}[1 \ 1 \ 1]^\dagger$ is given by

$$\begin{aligned} \hat{T}(k, l) &= \begin{bmatrix} 0 & \langle\alpha|\beta'(k, l)\rangle \\ \langle\beta'(k, l)|\alpha\rangle & 0 \end{bmatrix} \\ &= \frac{1}{3} \begin{bmatrix} 0 & 1 + e^{il} + e^{i(k+l)} \\ 1 + e^{-ik} + e^{-i(k+l)} & 0 \end{bmatrix}. \end{aligned}$$

$\hat{T}(k, l)$ is defined on the intersection graph and its spectrum is $\sigma(\hat{T}(k, l)) = \{\pm|1 + e^{il} + e^{i(k+l)}|/3\}$. Using Theorem 2, we obtain

$$\begin{aligned} \sigma(\hat{U}_\theta(k, l)|_{\mathcal{A}+\mathcal{B}}) &= \left\{ e^{i\eta} \mid \cos \eta = -1 + \frac{2}{3 \sin^2 \theta} + \frac{4}{9 \sin^2 \theta} (\cos l + \cos k + \cos(k+l)) \right\}, \\ \sigma(\hat{U}_\theta(k, l)|_{(\mathcal{A}+\mathcal{B})^\perp}) &= \{-e^{-2i\theta}\}. \end{aligned}$$

The eigenvectors of $\hat{U}_\theta(k, l)$ in $(\mathcal{A} + \mathcal{B})$ are obtained from the eigenvectors of $\hat{T}(k, l)$ and the eigenvectors in $(\mathcal{A} + \mathcal{B})^\perp$ are obtained using the cycle-path method. Let us focus on the latter. Let the set of edges of the quotient graph be $\{1, 2, 3\}$ as depicted in Fig. 3. The labeling can be converted to the notation of Section 4.3 by using $\{e_1, e_2, f_1\}$ and by identifying f_2 with e_2 . Since $\hat{T}(k, l)$ does not have (+1)-eigenvectors when $(k, l) \neq (0, 0)$, $\hat{T}(k, l)$ is nonreversible. The spanning tree of the intersection graph contains only one edge (take the one with label 2). There are two fundamental cycles: $c_0 = \{1, 2\}$ and $c = \{2, 3\}$. We use Case 2 of Proposition 2 in order to compute an eigenvector $\hat{\psi}_c^{c_0} \in \ker(e^{-2i\theta} + \hat{U}_\theta)$. We have $a(1) = a(2) = e(3) = 1/\sqrt{3}$ and $b(1) = 1/\sqrt{3}$, $b(2) = e^{il}/\sqrt{3}$, $b(3) = e^{i(k+l)}/\sqrt{3}$. We set $\hat{\psi}_c^{c_0}(1) = 1$, and using Eq. (4.21) we obtain $\hat{\psi}_c^{c_0}(2) = -e^{il}$. Using Eq. (4.29), we obtain $\hat{\psi}_c(3) = (e^{il} - 1)/(1 - e^{-ik})$ and then $\hat{\psi}_c(2) = (1 - e^{il})/(e^{ik} - 1)$. Adding vectors $\hat{\psi}_c^{c_0}$ and $\hat{\psi}_c$, we obtain $\hat{\psi}_c^{c_0} = (1, (e^{-ik} - e^{il})/(1 - e^{-ik}), (e^{il} - 1)/(1 - e^{-ik}))$, which is an eigenvector of $\hat{U}_\theta(k, l)$ with eigenvalue $(-e^{-2i\theta})$.

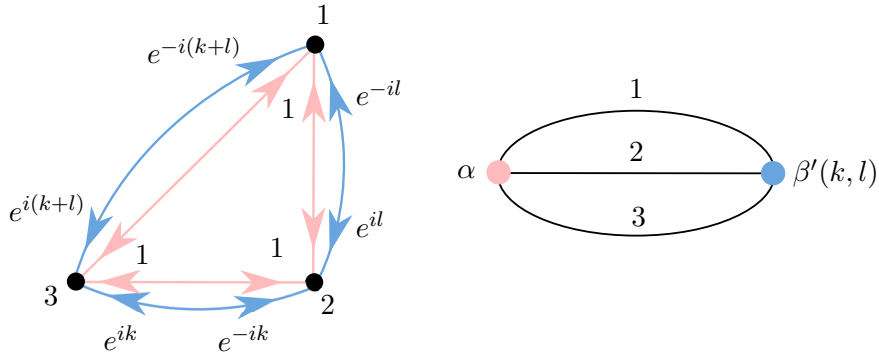


Figure 3: The left-hand graph is the quotient graph of the kagome lattice, which is a triangle with double edges. We have depicted the weights of the red and blue arcs. The right-hand graph is the intersection graph of the quotient graph. The labels of the edges are 1, 2, and 3.

By applying the inverse Fourier transform, the eigenvectors, which have finite support, are lifted up to the real space of the original graph G and are expressed by

$$\psi_{(x,y)}(x', y', j) = \begin{cases} 1 & \text{if } (x', y', j) = \{(x, y, 1), (x, y + 1, 3), (x - 1, y, 2)\}, \\ -1 & \text{if } (x', y', j) = \{(x, y, 3), (x, y + 1, 2), (x - 1, y, 1)\}, \\ 0 & \text{otherwise,} \end{cases}$$

for any $(x, y) \in \mathbb{Z}^2$. The support of $\psi_{(x,y)}$ is a 6-cycle of the kagome lattice. Note that if the initial state has overlap with any of these eigenvectors, there will be localization.

Acknowledgments

YuH's work was supported in part by Japan Society for the Promotion of Science Grant-in-Aid for Scientific Research (C) 25400208, (C) 18K03401 and (A) 15H02055. RP is grateful to the kind hospitality of the Graduate School of Information Sciences and Research Alliance Center for Mathematical Sciences (RACMaS), Tohoku University, which sponsored his visit during the winter of 2018. IS is partially supported by the Grant-in-Aid for Scientific Research (C) of Japan Society for the Promotion of Science (Grant No. 15K04985). ES acknowledges financial support from the Grant-in-Aid for Young Scientists (B) and of Scientific Research (B) Japan Society for the Promotion of Science (Grant No. 16K17637, No. 16K03939).

References

- [1] D. Aharonov, A. Ambainis, J. Kempe, and U. Vazirani. Quantum walks on graphs. In *Proc. 33th STOC*, pages 50–59, New York, 2001. ACM.
- [2] A. Ambainis. Quantum walk algorithm for element distinctness. In *Proc. 45th Annual IEEE Symposium on Foundations of Computer Science FOCS*, pages 22–31, Washington, 2004.
- [3] F. Cardano, F. Massa, H. Qassim, E. Karimi, S. Slussarenko, D. Paparo, C. De Lisio, F. Sciarrino, E. Santamato, R.W. Boyd, and L. Marrucci. Quantum walks and wavepacket dynamics on a lattice with twisted photons. *Science Advances*, 1(2):e1500087, 2015.

- [4] C. M. Chandrashekar, S. Banerjee, and R. Srikanth. Relationship between quantum walks and relativistic quantum mechanics. *Phys. Rev. A*, 81:062340, 2010
- [5] A. M. Childs. On the relationship between continuous- and discrete-time quantum walk. *Commun. Math. Phys.*, 294(2):581–603, 2010.
- [6] E. Farhi and S. Gutmann. Quantum computation and decision trees. *Phys. Rev. A*, 58:915–928, 1998.
- [7] M. Genske, W. Alt, A. Steffen, A. H. Werner, R. F. Werner, D. Meschede, and A. Alberti. Electric quantum walks with individual atoms. *Phys. Rev. Lett.*, 110:190601, 2013.
- [8] J. L. Gross and J. Yellen. *Graph Theory and Its Applications*. Chapman & Hall/CRC, Boca Raton, FL, 2005.
- [9] S. Gudder. Quantum Markov chain. *J. Math. Phys.*, 49(7):072105, 2008.
- [10] Yu. Higuchi, N. Konno, I. Sato, and E. Segawa. Spectral and asymptotic properties of Grover walks on crystal lattices. *J. Funct. Anal.*, 267(11):4197–4235, 2014.
- [11] Yu. Higuchi and T. Shirai. Some spectral and geometric properties for infinite graphs. *Contemp. Math.* 347:29–56, 2004.
- [12] C. Hoede. A characterization of consistent marked graphs. *J. Graph Theory*, 16(1):17–23, 1992.
- [13] T. Kitagawa, M. S. Rudner, E. Berg, and E. Demler. Exploring topological phases with quantum walks. *Phys. Rev. A*, 82:033429, 2010.
- [14] N. Konno, Y. Ide, and I. Sato. The spectral analysis of the unitary matrix of a 2-tessellable staggered quantum walk on a graph. *Linear Algebra Appl.*, 545:207–225, 2018.
- [15] N. Konno, R. Portugal, I. Sato, and E. Segawa. Partition-based discrete-time quantum walks. *Quantum Inf. Process.*, 17(4):100, 2018.
- [16] M. Kotani, T. Shirai, and T. Sunada. Asymptotic behavior of the transition probability of a random walk on an infinite graph. *J. Funct. Anal.*, 159:664–689, 1998.
- [17] D. Peterson. Gridline graphs: a review in two dimensions and an extension to higher dimensions. *Discrete Appl. Math.*, 126(2):223–239, 2003.
- [18] P. Philipp and R. Portugal. Exact simulation of coined quantum walks with the continuous-time model. *Quantum Inf. Process.*, 16(1):14, 2017.
- [19] R. Portugal. Staggered quantum walks on graphs. *Phys. Rev. A*, 93:062335, 2016.
- [20] R. Portugal, M. C. de Oliveira, and J. K. Moqadam. Staggered quantum walks with Hamiltonians. *Phys. Rev. A*, 95:012328, 2017.
- [21] R. Portugal, R. A. M. Santos, T. D. Fernandes, and D. N. Gonçalves. The staggered quantum walk model. *Quantum Inf. Process.*, 15(1):85–101, 2016.
- [22] N. Shenvi, J. Kempe, and K. B. Whaley. A quantum random walk search algorithm. *Phys. Rev. A*, 67(5):052307, 2003.

- [23] T. Shirai. The spectrum of infinite regular line graph. *Trans. Amer. Math. Soc.*, 352:115-132, 2000.
- [24] F. W. Strauch. Connecting the discrete- and continuous-time quantum walks. *Phys. Rev. A*, 74(3):030301, 2006.
- [25] T. Sunada. *Topological Crystallography: With a View Towards Discrete Geometric Analysis*. Springer, New York, 2013.
- [26] T. Sunada and T. Tate. Asymptotic behavior of quantum walks on the line. *J. Funct. Anal.*, 262, 2608–2645, 2012.
- [27] A. Suzuki. Asymptotic velocity of a position-dependent quantum walk. *Quantum Inf. Process.*, 15(1):103–119, 2016.
- [28] I. Syôzi. Statistics of kagomé lattice. *Progress of Theoretical Physics*, 6(3):306–308, 1951.
- [29] M. Szegedy. Quantum speed-up of Markov chain based algorithms. In *Proc. 45th Annual IEEE Symposium on Foundations of Computer Science, FOCS '04*, pages 32–41, Washington, 2004.